Chapter 1

Introduction

1.1 Historical exploration

Everyone in the present society is aware of their susceptibility to one or more illnesses including cancer, arthritis, asthma, hepatitis, tuberculosis, etc. Comparably, a structural element may be prone to one, two, or even many types of failure. A roller bearing, for instance, is most likely to fail after a particular number of rotations due to roller fatigue under certain load conditions. Most structural failures are often caused by one of the factors that fit into one of the following categories:

- Negligence in the structure's design, construction, or operation.
- Application of a novel design or material that yields an undesirable outcome.

The first type of failure, for which the suitable technology and experience are available to avert failure but are not employed due to human error, ignorance, or purposeful misconduct, includes errors in stress analysis, poor workmanship, and improper or subpar materials, and operator error.

It is significantly more challenging to avoid the second kind of failure. New materials may have many benefits, but they may also have drawbacks. As a result, a novel design or substance should only be put into use after thorough testing and study. This will reduce the frequency of failures, but not eliminate them. The brittle fracture of the Liberty ships during World War II is a well-known illustration of this sort of failure. These ships, which were the first to feature an all-welded hull, could be built much more quickly and affordably than earlier riveted designs, but the design change led to a considerable proportion of these vessels suffering major fractures. Today, almost all steel ships are welded, but the failures of the Liberty ship provided enough knowledge to prevent similar ones in the present structures.

Therefore, it is necessary to conduct fracture mechanics research to create convenient and efficient means of controlling structural failure. The foundation of fracture mechanics is the presumption that a work component has a crack in it. The crack may be a result of manufacturing flaws in a component or it may be man-made, such as a hole, notch, slot, etc. A few centuries prior, experiments conducted by Leonardo da Vinci (1452–1519) provided some hints as to the primary cause of fracture. When he tested the strength of iron wires, he discovered that the length of the wire affected the strength. Wohler [118] was one of the pioneering researchers (1860) who used controlled cyclic loads to study the fatigue of locomotive axels, which resulted in the development of the S-N diagram. In 1920, Griffith [45] presented a theory outlining a relationship between fracture stress and flaw size. According to the idea, when the material's surface energy exceeds the change in strain energy brought on by an increase in crack propagation, the flaw becomes unstable and leads to the fracture.

The United States created a new sort of ship during the early stages of World War II called the Liberty ship that had an entirely welded hull as opposed

to the conventional ships, which were constructed by riveting plates together. But shortly after, one of the Liberty ships split in two when traveling between Siberia and Alaska, demonstrating the problems with the welded structures of the ships [117]. As a result, many of these ships break down in the frigid temperature of the North Atlantic Ocean (see Figure 1.1).

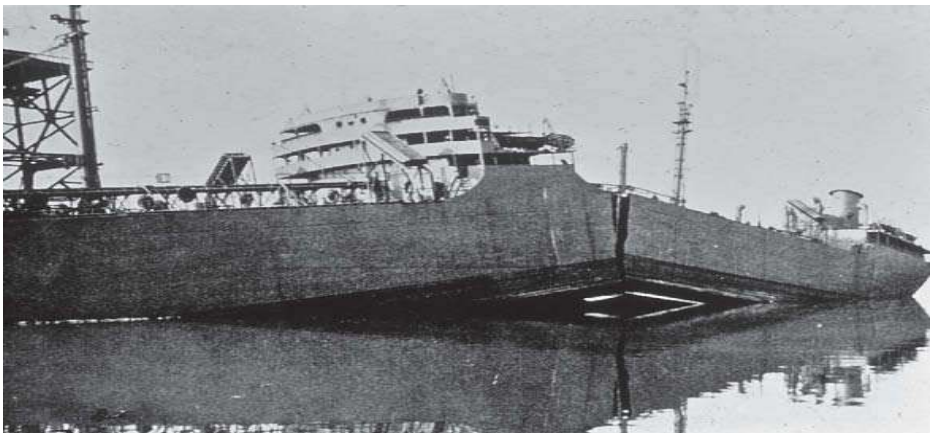

Figure 1.1: Cracked Liberty ship.

The failures of the Liberty ship were brought on by a combination of the following three factors during investigations:

- the welds have crack-like imperfections,
- the majority of the fractures started on the deck around square hatch corners, where there was a local stress concentration, and
- the steel used to construct the Liberty ships had low toughness.

A welded structure has a large single continuous part and therefore, if the crack becomes critical it will run through the entire hull of the ship. However, the ships made of riveting plates did not exhibit such failures because cracks could not propagate

across panels that were joined by rivets. Due to this incident, fracture mechanics becomes an engineering discipline rather than just a scientific curiosity.

In the decade following the war, a team of researchers at the Naval Research Laboratory in Washington, DC, under the guidance of Dr. G.R. Irwin, thoroughly investigated the fracture problem. Irwin [53] developed fracture mechanics by coming up with practical criteria like stress intensity factor and energy release rate. Other criteria, such as Crack Tip Opening Displacement, were introduced by Wells [114] in 1961 and J-Integral by Rice [96] in 1968. Several successful early applications of fracture mechanics bolstered the standing of this new field in the engineering community.

1.2 Modes of fracture failure

A line with varying curvature typically represents the crack front in a structural component. Consequently, varying loading arrangements close to the crack result in distinct modes of crack tip surface displacements. According to Figure 1.2, the three fundamental loading configurations result in Mode I, Mode II, and Mode III, the three fundamental fracture modes of crack tip deformation.

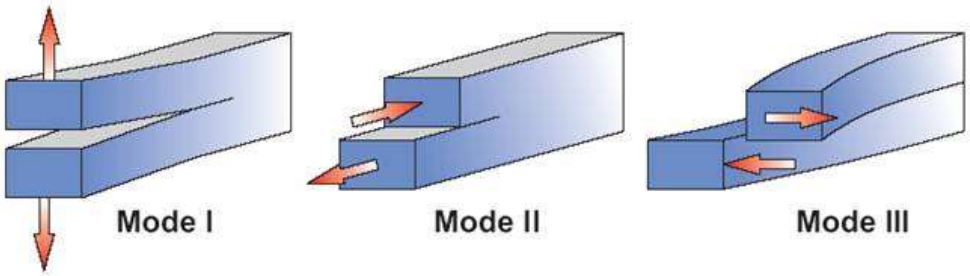

Figure 1.2: Different modes of fracture.

- **Mode I** is the opening (or tensional) mode. In this mode, the crack faces separate at the crack front and the load applied to the crack tip is normal to the crack plane, causing the displacements of the crack surfaces to be perpendicular to the crack plane.

- **Mode II** is the edge-sliding mode (or in-plane shearing) in which the crack tip is subjected to in-plane shear loading and the crack faces slide relative to each other, causing crack surface displacements to be in the crack plane and perpendicular to the crack front.

- **Mode III** is the tearing (or out of plane) mode. An anti-plane shear loading is applied to the crack tip. The displacements of the crack surfaces are in the crack plane but parallel to the crack front as a result of relative movement between the crack faces.

In a **Mixed-mode** problem more than one loading mode is present.

1.3 Fracture mechanics approach to design

Figure 1.3 illustrates how the fracture mechanics approach to design differs from the conventional strength of materials approach. According to the strength of materials approach, a material is considered adequate if its strength exceeds the anticipated applied stress. Three factors are involved in the fracture mechanics approach: applied stress, fault size, and fracture toughness. The energy and stress intensity approaches are two alternate methods for fracture analysis. The next sections provide a thorough discussion of those.

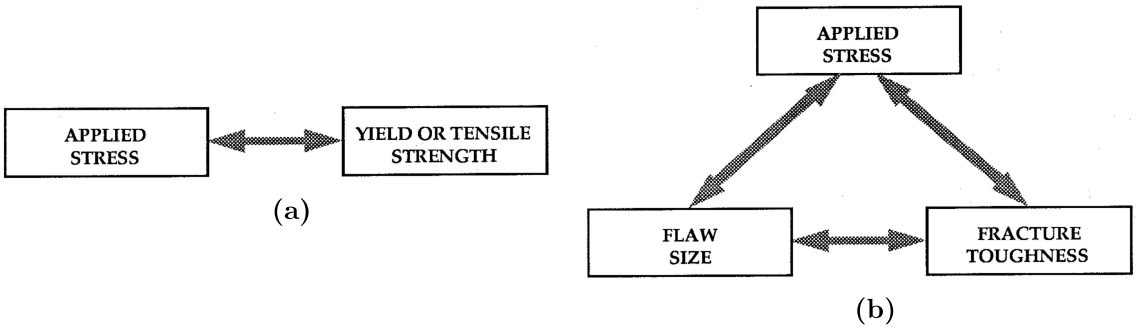

Figure 1.3: Comparison between (a) strength of materials approach and (b) fracture mechanics approach.

1.3.1 Energy approach

The energy approach for fracture was first proposed by A. A. Griffith [45], but it was Irwin who developed the concept [54]. A. A. Griffith postulated that a crack in a body would not grow unless energy was released to overcome the energy required for forming two new surfaces, one below and one above the crack plane. Thus, the energy method has two crucial quantities viz., (i) the amount of energy released as a crack advances (ii) the minimum energy needed for a crack to advance for producing two new surfaces.

Energy release rate (ERR) is used to measure the first quantity, which is represented by G after Griffith. ERR is defined as energy release per unit increase in the area during crack growth. Crack resistance, which is typically represented by the symbol R, is the amount of energy needed for a crack to grow per unit area extension. The energy release rate is the driving force for fracture, whereas the material's resistance to fracture is known as crack resistance. To investigate the potential of a crack becoming critical, both of these rates are required.

1.3.2 Stress intensity factor approach

It is possible to obtain closed-form expressions for the stresses in the body for isotropic linear elastic material behavior and specific cracked configurations subjected to external forces. These solutions were first published by Westergaard [115], Irwin [55], Sneddon [106], and Williams [116]. An element near the tip of a crack in an elastic material, as well as the in-plane stresses on this element, are schematically depicted in Figure 1.4.

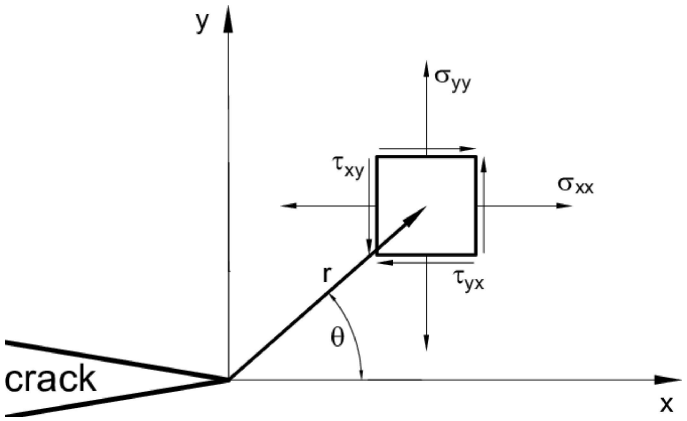

Figure 1.4: The coordinate axis ahead of a crack tip for normal z-direction.

Thus, it can be demonstrated that the stress field in any linear elastic cracked body is determined by setting a polar coordinate axis with the origin at the crack tip as

$$\sigma_{ij} = \frac{K}{\sqrt{2\pi r}} f_{ij}(\theta) + \sum_{m=0}^{\infty} A_m r^{\frac{m}{2}} g_{ij}^{m}(\theta), \tag{1.1}$$

where σ_{ij} is the stress tensor, K is a constant, f_{ij} is dimensionless function of θ in the leading term, and for higher order terms A_m is the amplitude and g_{ij}^{m} is a dimensionless function of θ for the m^{th} term. The solution for any configuration comprises a leading term that is proportional to $1/\sqrt{r}$, but the higher-order terms

depend on geometry. While the other terms remain finite or approach to zero as $r \to 0$, with the leading term approaches infinity. Thus, regardless of how the cracked body is configured, the stress in the vicinity of the crack tip varies with the $1/\sqrt{r}$ singularity, but the proportionality constants K and fij rely on the mode.

It should be noted that each stress component is proportional to a constant K. Knowing this constant allows one to determine the complete stress distribution at the crack tip. This constant is referred to as the stress-intensity factor (SIF). The crack-tip conditions in a linear elastic material are entirely characterized by SIF. The different modes of fracture are typically identified by a subscript, such as K_I, K_{II}, and K_{III} for Modes I, II, and III, respectively. The separate contributions to a specific stress component in a mixed-mode problem are additive. Equation (1.1) clearly shows that SIF has units of $stress * \sqrt{length}$, where the only pertinent length scale is crack size.

The fracture must happen at a critical stress intensity K_{Ic} if one considers that the material fails locally at some critical combination of stress and strain. Consequently, an alternate way to assess fracture toughness is K_{Ic}. When $K = K_{Ic}$, failure happens. In this scenario, the driving force for fracture is K, while the resistance of the material is measured by K_{Ic}.

1.4 Hooke's law

The law of elasticity known as Hooke's law was proposed by Robert Hooke in 1676. According to this, the produced deformation is proportional to the load that causes it. Stress is a linear function of strain, this is how the law can be phrased in terms

of stress. This is also referred to as the Generalised Hooke's law. Thus,

$$\text{stress } = \mu * \text{ strain}, \tag{1.2}$$

where μ is the proportionality constant, known as the modulus of elasticity.

1.5 Functionally graded material

Since the first man arrived on earth, the materials have been playing a significant part in human life. Man has utilized distinct materials or composites in different eras for a variety of applications due to their versatility. At first, bronze, an alloy of tin and copper, was widely utilized. Once iron was found, people continued to be interested in using it to create a variety of items. Following that, a wide variety of metal and nonmetal alloys were developed for numerous applications. Due to their numerous applications, composite materials then attracted a lot of attention from researchers. Composite materials can offer design flexibility and are both lighter and stronger. They offer resistance to wear as well as corrosion. The drawback of composite materials is a sharp transition in characteristics at the material junction, which causes a component to fail through the delamination process.

One of the biggest obstacles in developing novel materials in today's extremely demanding technological world is combining seemingly incompatible thermomechanical properties into a single component (e.g., high heat and corrosion resistance, high strength in elevated-temperature applications, and high resistance to wear, and high toughness in load-bearing elements). In many instances, the issue can be resolved by applying coatings or by overlaying disparate materials. The resultant high thermal and residual stresses and relatively weak bonding strength

have been a significant drawback of these techniques from a structural standpoint, notably in the ceramic coating of metals. Therefore, surface cracking and debonding or delamination have been frequent types of mechanical failure in thin films, coatings, and layered materials. Eliminating material property discontinuities by grading the material composition near the interfaces or through the coating has proven to be an efficient technique to reduce residual and thermal stresses and enhance the bonding strength. These novel materials, with continuously varying compositions or volume fractions, are referred to as functionally graded materials (FGMs). FGMs are essentially two-phase particle composites that have been created in a way that causes the volume fractions of the elements to fluctuate continuously in the thickness direction to produce a predetermined composition profile [50, 62]. In turn, the composition profile is chosen so that the resulting nonhomogeneous material exhibits the required thermomechanical properties, ranging from 0% ceramic at the interface to 100% close to the surface. Japanese scientists created the first of this new breed of composite materials in 1984 for the core purpose of their aerospace project [87], which called for a thermal barrier with an exterior temperature of 2000 k and an interior temperature of 1000 k within 10 mm thickness.

The physical, chemical, and mechanical properties of the material, such as Young's modulus, Poisson's ratio, shear modulus, density, and coefficient of thermal expansion in a specified spatial direction, are replaced by FGMs with smooth and continuous fluctuating properties instead of sharp transitions [1, 29, 41, 82]. The gradual changes in volume fraction of constituent and nonidentical structure at the preferred direction give continuously graded properties like thermal conductivity, corrosion resistivity, specific heat, hardness, and stiffness ratio [2]. Due to all these benefits, FGMs are considerably superior to homogenous composite materials for use in various applications. Although the initial research on FGMs was primarily driven

by the practical applications of the concept in a wide variety of thermal shielding problems, materials with graded physical properties offer unlimited potential in many other technological applications. It has so far been applied to practically every sector, including the biomedical, chemical, nuclear, mining, and power plant sectors (see Figure 1.5). FGMs are found in nature in the form of bones, teeth, bamboo

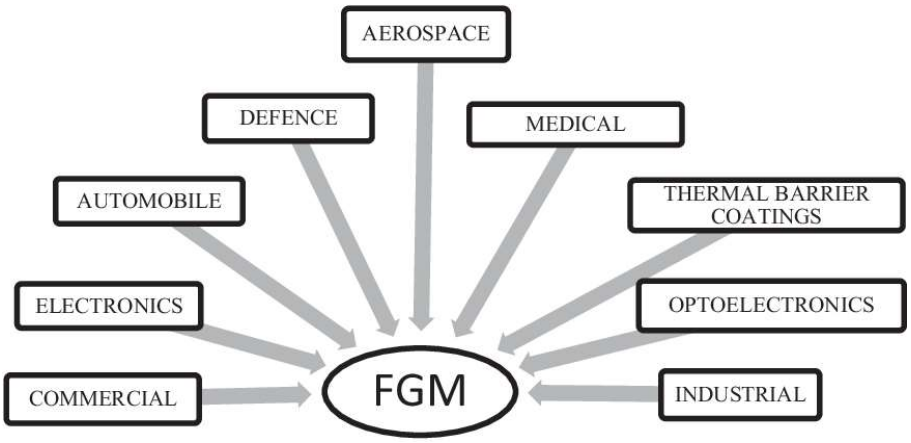

Figure 1.5: Applications of FGM.

plants, human skin, and other structures to satisfy the requirements of both humans and the environment.

The major purpose of mechanics research on FGMs is to offer technical assistance to material scientists and design and manufacturing engineers. FGMs are quite new and yet in the early stages of development. Fundamental investigations into these materials' mechanics must be done in conjunction with studies on their processing to fully exploit their beneficial features in the development of new products. From a mechanical perspective, the distinctive quality of FGMs is that they exhibit nonhomogeneity in terms of both their thermomechanical properties as well as their strength-related characteristics, such as yield strength, fracture toughness, fatigue, and creep behavior. For FGMs, a considerable bulk of research is devoted to examining how different failure modes are affected by material nonhomogeneity.

1.6 Literature survey

The failure of FGMs owing to fracture is a serious problem that must be addressed. When subjected to high-temperature loading conditions, FGMs can develop a variety of crack forms. Some key notions about FGMs and their fracture-related issues were explored in [33]. Embedded cracks in non-homogeneous media possess the typical square-root singularity, as proved by [64] and [88]. Several difficulties have already been solved for FGMs subjected to thermal, mechanical, and thermo-mechanical loads. An embedded crack parallel to the free surface and exposed to continuously variable thermal properties in an infinite FGM material was investigated in [88]. Steady-state heat flux was applied to the crack surface. [8] extended the same problem to a partially insulated crack where the heating source is located far from the crack zone, and a crack-closure algorithm is also presented there. [59] investigated the interface crack problem with ceramic and/or FGM coatings and a substrate under anti-plane shear loading for different coating models. In [51], a new model was proposed for the approximation analysis of FGMs with arbitrary variable properties and to address the issue of a fracture in a functionally graded coating adhered to a homogeneous substrate under static anti-plane shear loading. The steady-state heat flow problem for a crack perpendicular to the graded interfacial zone in bonded media was discussed in [17].

Crack interaction is an important factor to consider while investigating fundamental crack difficulties in graded materials. In [93], the problem of collinear cracks in an inhomogeneous orthotropic medium under mode I plane strain and plane stress loading conditions were investigated for cracks positioned in a plane and parallel to the direction of material property variations under external loads. [89] investigated the subject of collinear cracks in FGMs under thermal loading. [94] investigates the thermal fracture problem for a functionally graded strip, and an

analytical model for collinear cracks is developed using the piezoelectric model and steady-state temperature field. [95] studied the interplay of a system of edge cracks in a functionally graded coating on a homogenous substrate. [31] gave a theoretical approach for two anti-plane collinear cracks perpendicular to and on either side of the interface between a functionally graded orthotropic strip and an orthotropic homogeneous substrate.

Recently, researchers have concentrated on the dynamic behavior of fracture problems in non-homogeneous materials. In [122], dynamic analysis for a finite-length crack in the FGMs under harmonic stress waves was provided utilizing the Schmidt method. The effect of non-homogeneous elastic constants on DSIFs for an interfacial crack was studied in [67]. DSIFs for a FGM fracture implanted between two elastic layers while subjected to anti-plane loading were determined in [66]. A theoretical description of the dynamic behavior of a Griffith crack in functionally graded orthotropic materials under the normal incidence of time-harmonic elastic waves was provided in [71]. Recently, researchers have concentrated on the dynamic behavior of single crack problems in non-homogeneous materials, but less research has been done on the corresponding multiple crack problems and their interactions under impact loads applied to the material surface. The Schmidt technique was used in [72] to analyze the dynamic behavior of two collinear cracks in a FGM layer joined to different half-planes. [68] considered an anti-plane dynamic fracture with two collinear cracks perpendicular to a weak discontinuous interface point between two elastic materials.

The investigations listed above concentrated on cracks that are either parallel or vertical to an interface or surface. However, these crack positions are extremely particular. It is crucial to investigate arbitrarily oriented crack problems in FGMs. The heat conduction problem for an angled crack in an infinite functionally graded

material was investigated in [16]. In the investigation, the nature of the crack is believed to be partially insulated under a uniform heat flow. [110] investigated a similar problem with a fully insulated crack. In each of these investigations, the crack is placed in an infinite functionally graded material. The fracture problem of a crack in functionally graded strips in the presence of mechanical loading was inspected in [47], in which the possibility of crack passing through the interface of the said composite structure is also discussed along with the study of SIF for different material non-homogeneity constants, normalized crack length, and orientation angle. A similar problem was investigated for an arbitrary-oriented fracture in [49]. The concept of dislocation density functions was used to determine the unknowns in this research.

1.7 Foundation for mathematical analysis

This section would lay the mathematical foundation for tackling fracture problems. The solution to fracture problems would be obtained by solving field equations of solid mechanics. There are three different types of field equations that are resolved for a particular set of boundary conditions for a component [107]. Those are as follows:

1. equilibrium equations relating to stress components,
2. strain-displacement relations, and
3. stress-strain relations for the chosen material of the component.

To ensure that a continuous body remains continuous during the deformation, additional equations must be satisfied for problems solved by employing stress or strain

components as dependent variables. Compatibility is the term used to describe this condition [42]. The governing differential equations for many problems are provided by the compatibility condition.

1.7.1 Equilibrium equation

Equilibrium equations include the two differential equations listed below:

$$\frac{\partial \sigma_{xx}}{\partial x} + \frac{\partial \sigma_{xy}}{\partial y} = 0 \quad \text{and} \quad \frac{\partial \sigma_{xy}}{\partial x} + \frac{\partial \sigma_{yy}}{\partial y} = 0. \tag{1.3}$$

1.7.2 Strain-displacement and compatibility relations

If u and v are displacement components, ϵ_{xx}, ϵ_{xy} and ϵ_{yy} are strain components then the strain-displacement relations are as follows:

$$\epsilon_{xx} = \frac{\partial u}{\partial x}, \quad \epsilon_{yy} = \frac{\partial v}{\partial y}, \quad \text{and} \quad \epsilon_{xy} = \frac{1}{2}\left[\frac{\partial v}{\partial x} + \frac{\partial u}{\partial y}\right]. \tag{1.4}$$

By removing u and v from equation (1.4), the compatibility condition is obtained. Compatibility is ensured by the following relationship between strain components.

$$\frac{\partial^2 \epsilon_{xx}}{\partial y^2} + \frac{\partial^2 \epsilon_{yy}}{\partial x^2} - 2\frac{\partial^2 \epsilon_{xy}}{\partial x \partial y} = 0. \tag{1.5}$$

1.7.3 Stress-strain relation

The following is the stress-strain relation for linear isotropic materials deforming elastically:

$$\epsilon_{xx} = \frac{1}{E}[\sigma_{xx} - \nu(\sigma_{yy} + \sigma_{zz})], \tag{1.6}$$

$$\epsilon_{yy} = \frac{1}{E}[\sigma_{yy} - \nu(\sigma_{xx} + \sigma_{zz})], \tag{1.7}$$

$$\epsilon_{zz} = \frac{1}{E}[\sigma_{zz} - \nu(\sigma_{xx} + \sigma_{yy})], \tag{1.8}$$

$$\epsilon_{xy} = \frac{(1+\nu)}{E}\sigma_{xy}, \tag{1.9}$$

where E is Young's Modulus and ν is the Poisson's ratio.

In plane stress, a thin plate gets deformed. As a result, out-of-plane strains are zero on free surfaces and are often insignificant at interior points of the plate. As a result,

$$\sigma_{xz} = \sigma_{yz} = \sigma_{zz} = 0. \tag{1.10}$$

On the other hand, the plane strain case corresponds to a sufficiently thick plate, wherein variation is zero and displacement is restricted in the z-direction. These two conditions yield

$$\epsilon_{xz} = \epsilon_{yz} = \epsilon_{zz} = 0. \tag{1.11}$$

1.8 Mathematical methods and techniques

1.8.1 Integral equation

An equation involving an unknown function $\phi(x)$ and if $\phi(x)$ appears under the sign of integration, the equation is said to be an integral equation for $\phi(x)$ with $a \leq x \leq b$

(a, b being real constants). For instance the equations

$$\lambda \int_a^b K_1(x,t)\phi_1(t)dt = f_1(x), \tag{1.12}$$

$$\phi_2(x) + \int_a^x K_2(x,t)\phi_2(t)dt = f_2(x), \tag{1.13}$$

$$g(x)\phi_3(x) + \int_a^b K_3(x,t)\left[\phi_3(t)\right]^2 dt = 0, \tag{1.14}$$

where $K_1(x,t)$, $K_2(x,t)$, $K_3(x,t)$, $f_1(x)$, $f_2(x)$, $g(x)$ are known functions, $\phi_1(x)$, $\phi_2(x)$, $\phi_3(x)$ are unknown functions, λ is a constant and $x \in [a,b]$, are all integral equations.

The known function $K_i(x,t)$ $(i = 1,2,3)$ is referred to as the kernel of the integral equation and the other known function $f_i(x)$ $(i = 1,2)$ is considered as the forcing term of the associated integral equation. When the forcing term is non-zero, an integral equation is referred to as a non-homogeneous integral equation while if the forcing term is zero, the integral equation is referred to as a homogeneous integral equation. For instance, the integral equations (1.12) and (1.13) indicate non-homogeneous integral equations while the integral equation (1.14) represents a homogeneous integral equation.

A linear integral equation is one in which the unknown function is expressed linearly; on the other hand, a non-linear integral equation is one in which the unknown function is expressed non-linearly. For example, the integral equations (1.12) and (1.13) are linear integral equations while the integral equation (1.14) is a non-linear integral equation.

If both of the integration limits a and b are constants, the corresponding integral equation is said to be of the Fredholm type. If only one of the integration limits, a or b, is a known function of x, the associated integral equation is said to be

of Volterra type. The integral equations (1.12) and (1.14) are examples of integral equations of the Fredholm type, whereas the integral equation (1.13) is an example of Volterra type integral equation.

The integral equation is considered to be of the first kind if the known function $g(x) = 0$. In the case of $g(x) = 1$, the integral equation is said to be of the second kind, and in the case of $g(x) \neq 0$, it is of the third kind. The integral equations (1.12), (1.13) and (1.14) are first, second and third kind integral equations, respectively.

1.8.2 Singular integral equation

The integral equation is said to be the singular integral equation if either one or both integration limits become infinite or the kernel becomes infinite at one or more points within the integration's range. The integral equations shown below are examples of singular integral equations.

$$\phi_4(x) = f(x) + \lambda \int_{-\infty}^{\infty} \exp^{-|x-t|} \phi_4(t) dt, \tag{1.15}$$

$$f(x) = \int_0^x \frac{\phi_5(t)}{(x-t)^\alpha} dt, \quad 0 < \alpha < 1, \tag{1.16}$$

1.8.3 Laplace transform

Let $f(t)$ be a real-valued function with a range of values between $(-\infty, \infty)$ such that $f(t) = 0, \ \forall \ t < 0$. Assume that $f(t)$ is of exponential order as $t \to \infty$ and piecewise continuous in every finite interval. If so, the Laplace transform $f^*(p)$ of

$f(t)$ exists and is defined as

$$f^*(p) = \int_0^\infty \exp(-pt)\ f(t)dt, \tag{1.17}$$

where the parameter p is a real or complex number.

1.8.4 Inverse Laplace transform

The Laplace transform of $f(t)$ under the stated conditions is $f^*(p)$, as was discussed in the preceding section. An inverse Laplace transform of $f^*(p)$ is denoted by $f(t)$, which is defined as

$$f(t) = \frac{1}{2\pi\iota} \int_{C-\iota\infty}^{C+\iota\infty} \exp(pt)\ f^*(p)dp, \tag{1.18}$$

where C is a real number used to avoid integration outside the reion of convergence. It must be greater than the real part of every singularity.

1.8.5 Fourier transform

Suppose $f(x)$ be a function defined over the interval $(-\infty, \infty)$ such that it meets the following Dirichlet's conditions.

1. $f(x)$ is absolutely integrable over the defined interval,
2. $f(x)$ has a finite number of maxima and minima in every finite interval, and
3. $f(x)$ has a finite number of discontinuities in every finite interval and each of these discontinuities is finite.

The Fourier transform $\overline{f}(\tau)$ of $f(x)$ thus exists and is defined by

$$\overline{f}(\tau) = \frac{1}{2\pi} \int_{-\infty}^{\infty} f(x) \exp(-i\tau x)\, dx. \tag{1.19}$$

Similar to this, the Fourier sine transform $\overline{f_s}(\tau)$ and Fourier cosine transform $\overline{f_c}(\tau)$ of $f(x)$ over the range $(0, \infty)$ are stated as

$$\overline{f_s}(\tau) = \frac{2}{\pi} \int_{0}^{\infty} f(x) \sin(\tau x)\, dx, \tag{1.20}$$

$$\overline{f_c}(\tau) = \frac{2}{\pi} \int_{0}^{\infty} f(x) \cos(\tau x)\, dx, \tag{1.21}$$

respectively.

1.8.6 Inverse Fourier transform

According to the aforementioned section, the Fourier transform, Fourier sine transform and Fourier cosine transform of $f(x)$ under the specified conditions are $\overline{f}(\tau)$, $\overline{f_s}(\tau)$ and $\overline{f_c}(\tau)$ respectively. The inverse Fourier transform of $\overline{f}(\tau)$ is defined as

$$f(x) = \int_{-\infty}^{\infty} \overline{f}(\tau) \exp(i\tau x)\, d\tau. \tag{1.22}$$

In a similar manner, the inverse Fourier sine transform of $\overline{f_s}(\tau)$ is given as

$$f(x) = \int_{0}^{\infty} \overline{f_s}(\tau) \sin(\tau x)\, d\tau, \tag{1.23}$$

and the inverse Fourier cosine transform of $\overline{f_c}(\tau)$ is defined as

$$f(x) = \int_{0}^{\infty} \overline{f_c}(\tau) \cos(\tau x)\, d\tau. \tag{1.24}$$

1.8.7 Jacobi polynomial and related properties

A family of orthogonal polynomials with respect to the weight function $(1-x)^{\alpha}(1+x)^{\beta}$ on the interval $[-1,1]$ is known as Jacobi polynomials. In other words, Jacobi polynomial $P_n^{(\alpha,\beta)}(x)$ is a family of orthogonal polynomials with respect to the weight function $(1-x)^{\alpha}(1+x)^{\beta}$ on the interval $[-1,1]$. $P_n^{(\alpha,\beta)}(x)$ of degree n is defined as

$$P_n^{(\alpha,\beta)}(x) = \frac{1}{2^n n!}(1-x)^{-\alpha}(1+x)^{-\beta}\frac{d^n}{dx^n}\left[(1-x)^{\alpha}(1+x)^{\beta}(1-x^2)^n\right], \tag{1.25}$$

where $\alpha, \beta > -1$ and $x \in (-1,1)$.

Jacobi polynomials are generalizations of a number of families of orthogonal polynomials, including the first and second kinds of Chebyshev polynomials, the Legendre polynomial, and the Gegenbauer polynomial.

In fact, if $\alpha = \beta = -1/2$, then $P_n^{(-\frac{1}{2},-\frac{1}{2})}(x) = \frac{(2n)!}{2^{2n}(n!)^2}T_n(x)$, where $T_n(x)$ signifies the n^{th} Chebyshev polynomial of the first kind. With regard to the weight function $(1-x^2)^{-1/2}$ on the interval $(-1,1)$, the polynomials $\{T_n(x)\}_{n=0}^{\infty}$ are orthogonal.

If $\alpha = \beta = 1/2$, then $P_n^{(\frac{1}{2},\frac{1}{2})}(x) = \frac{(2n+2)!}{2^{2n+1}((n+1)!)^2}U_n(x)$, where $U_n(x)$ is the n^{th} Chebyshev polynomial of the second kind. The polynomials $\{U_n(x)\}_{n=0}^{\infty}$ are orthogonal with reference to the weight function $(1-x^2)^{1/2}$ on the range $(-1,1)$.

If $\alpha = \beta = 0$, then $P_n^{(0,0)}(x) = P_n(x)$, where $P_n(x)$ denotes the n^{th} Legendre polynomial. The polynomials $\{P_n(x)\}_{n=0}^{\infty}$ are orthogonal with respect to the weight function 1 on the interval $(-1,1)$.

If $\alpha = \beta = \nu - 1/2$ where $\nu > -1/2$ and $\nu \neq 0$, then $P_n^{(\nu-\frac{1}{2},\nu-\frac{1}{2})}(x) = \frac{(\nu+\frac{1}{1})_n}{(2\nu)_n}C_n^{\nu}(x)$, where $C_n^{\nu}(x)$ stands for the n^{th} Gegenbauer polynomial. The polynomials $\{C_n^{\nu}(x)\}_{n=0}^{\infty}$ are orthogonal for the choice of the weight function as $(1-x^2)^{\nu-1/2}$

on the range $(-1, 1)$.

The followings are some crucial points regarding the Jacobi polynomial:

Differential equation: The solution of the second order linear homogeneous differential equation

$$(1-x^2)y'' + (\beta - \alpha - (\alpha+\beta+2)x)y' + n(n+\alpha+\beta+1)y = 0. \tag{1.26}$$

is given by $P_n^{(\alpha,\beta)}(x)$.

Generating function: The generating function of the Jacobi polynomial is defined as

$$\sum_{n=0}^{\infty} P_n^{(\alpha,\beta)}(z)t^n = 2^{\alpha+\beta}R^{-1}(1-t+R)^{-\alpha}(1+t+R)^{-\beta}, \tag{1.27}$$

where $R = R(z,t) = (1-2zt+z^2)^{1/2}$.

Derivatives: The k^{th} derivative of the $P_n^{(\alpha,\beta)}(x)$ is obtained by using

$$\frac{d^k}{dz^k}P_n^{(\alpha,\beta)}(x) = \frac{\Gamma(\alpha+\beta+n+1+k)}{2^k\Gamma(\alpha+\beta+n+1)}P_{n-k}^{\alpha+k,\beta+k}(x), \tag{1.28}$$

Orthogonality condition: The following orthogonality condition is met by the Jacobi polynomial:

$$\int_{-1}^{1}(1-x)^{\alpha}(1+x)^{\beta}P_m^{(\alpha,\beta)}(x)P_n^{(\alpha,\beta)}(x)dx = \frac{2^{\alpha+\beta+1}}{2n+\alpha+\beta+1}\frac{\Gamma(n+\alpha+1)\Gamma(n+\beta+1)}{\Gamma(n+\alpha+\beta+1)n!}\delta_{nm}. \tag{1.29}$$

Symmetry relation : The symmetry relation of $P_n^{(\alpha,\beta)}(x)$ is expressed as

$$P_n^{(\alpha,\beta)}(-x) = (-1)^n P_n^{(\alpha,\beta)}(x). \tag{1.30}$$

1.8.8 Dirac delta function

The Dirac delta function $\delta(*)$ introdced by the physicist Paul Dirac is a generalized function that is formally defined as an integral

$$\int_{-\infty}^{\infty} f(x)\delta(x)dx = f(0), \tag{1.31}$$

for any continuous compactly supported function $f(x)$.

It can be conceptualized as a function on the real line that is zero everywhere but infinite at the origin, i.e.,

$$\delta(x) = \begin{cases} \infty & x = 0, \\ 0, & x \neq 0, \end{cases} \tag{1.32}$$

and additionally bound to satisfy $\int_{-\infty}^{\infty} \delta(x)\, dx = 1$.

1.8.9 Heaviside function

The Heaviside function $H(*)$ is a discontinuous function defined as

$$H(x) = \begin{cases} 1, & x \geq 0, \\ 0, & x < 0. \end{cases} \tag{1.33}$$

****